Department of Veterans Affairs

Journal of Rehabilitation Research and Development Vol. 38 No. 1, January/February 2001
Pages 57–68

A comparison of methods to compute the point of force application in handrim wheelchair propulsion: a technical note

Michelle B. Sabick, PhD; Kristin D. Zhao, MS; Kai-Nan An, PhD
Orthopedic Biomechanics Laboratory, Department of Orthopedics, Mayo Clinic/Mayo Foundation, Rochester, MN 55905

Abstract—Several methods are available for computing the location of the point of force application (PFA) in manual wheelchair propulsion using kinetic data. We compared five different techniques for computing the PFA location in analysis of data from five wheelchair users propelling their own wheelchairs using their normal propulsion style. The effects of the assumptions used in the calculations on the resulting location of the PFA, handrim force and moment components, and mechanical efficiency (*e*) were quantified. When kinetic data were used to locate the PFA, the most consistent and stable results were obtained using the assumptions that components of the handrim moment about the anteriorly directed and vertically directed axes were negligible. Some assumptions led to unsolvable equations at points during the propulsion cycle, demonstrating that they were inappropriate. All PFA values calculated with kinetic data were unstable at the beginning and end of the propulsion phase. While differences exist due to individual technique, assuming handrim moment components about the anterior-posterior, vertical, and/or both axes resulted in the most representative results.

This material is based on work supported by NIH grants HD33806 and HD07447.

Address all correspondence and requests for reprints to: Kai-Nan An, PhD, Mayo Clinic/Mayo Foundation, 128 Guggenheim Building, 200 First Street SW, Rochester, MN 55905; email: An.Kainan@mayo.edu.

Key words: *biomechanics, upper limb, wheelchair.*

INTRODUCTION

Handrim wheelchair propulsion has been implicated as a contributor to several overuse injuries of the upper limbs (1–4). Injury of the upper limb can be devastating to a wheelchair user who relies on the upper limbs for completing activities of daily living and also for mobility. Therefore, studies of wheelchair propulsion biomechanics as it relates to upper-limb loading are necessary. The goal of such studies is to identify inefficiencies in wheelchair- propulsion technique or motions likely to result in injury, so that they can be reduced or eliminated.

Estimates of mechanical efficiency (*e*) during propulsion have been obtained by calculating the ratio of the magnitude of the tangential force component to the magnitude of the resultant force applied to the wheel (5–7). The rationale for such calculations is that the tangential component of force is the only force component that aids in the propulsion of the wheelchair. The radial and normal (or axial) components of handrim force are useful only in that they provide the necessary friction

force to enable propulsion. Force in the radial or normal directions above that needed to generate frictional forces at the handrim is wasted in terms of wheelchair propulsion *e*.

Forces applied to the wheelchair handrim are generally recorded in a global x-y-z coordinate system. To calculate the magnitude of force components in the radial-tangential-normal (r-t-n) coordinate system for quantifying *e*, a point on the handrim that best represents the location where the force is being applied must be identified. This point is called the point of force application (PFA), and is similar to the center of pressure in gait studies. The tangential force component is along the line tangent to the handrim at the PFA. The radial and normal force components are defined based on the location of the PFA relative to the center of the wheel. Because the location of the PFA determines the radial and tangential directions, it affects the magnitudes of the radial and tangential force and moment components that are calculated. This, in turn, leads to differences in calculations of mechanical *e*. Therefore, the method used to determine PFA might affect the results of a study or the recommendations given to a wheelchair user to improve his or her technique.

In gait studies, force platforms can be used to solve a system of equations locating the center of pressure because only one component of moment (about the vertical axis) can be applied to the force platform by the foot. In manual wheelchair propulsion, however, the wheelchair user grips the handrim, and therefore can potentially apply a moment about any of the coordinate axes. While several different groups have developed instrumented pushrims to measure the force and moment components at the wheel axle (8–12), none has succeeded in instrumenting the handrim sufficiently to solve the system of equations locating the PFA directly. Therefore, assumptions must be made to decrease the number of unknowns so that a solution can be reached.

Determining the location of the PFA in handrim wheelchair propulsion has traditionally been done one of two ways: 1) using kinematic data, by assuming that the PFA is located at one of the metacarpophalangeal (MCP) joints; or 2) using kinetic data, by assuming that one or more of the handrim moment components applied is negligible, and calculating the location of the PFA from force data collected at the wheel hub (13). Both of the methods used to locate the PFA involve one or more assumptions, but the relative benefits of one technique over the other have not been clearly established, because there is no gold standard with which to compare.

Several authors have studied extensively the calculation, both in two dimensions and in three dimensions, of the PFA (13–16). The location of the PFA calculated from kinetic data has been shown to move within the hand, or even leave the hand, throughout the propulsion phase, suggesting that choosing a static location for the PFA within the hand (such as one of the MCP joints) is not appropriate (13,14). However, a tendency for the PFA calculated from kinetic data to become unstable near the beginning and end of the propulsion phase has also been described (13,14), while the location of the PFA remains stable when assumed to rest at one of the MCP joints (13). In fact, the location of the PFA can have an uncertainty of 100 percent at the beginning and end of the stroke cycle (15), suggesting it may be of limited use in some portions of the propulsion phase.

While the use of kinetic data to compute the location of the PFA has been recommended over the use of kinematic data (13), there are several methods that may be used to calculate the location of the PFA using kinetic data, each involving a different set of assumptions. To date, the superiority of one method over the other has not been clearly established. The purpose of this study was to quantify the differences between methods by comparing the effects of different assumptions on the calculated location of the PFA and the resulting handrim force and moment data. This comparison was made to determine the relative strengths and weaknesses of each assumption when locating the PFA during handrim wheelchair propulsion, and to recommend which calculation method is most appropriate for use in calculations of wheelchair-propulsion *e*.

METHODS

Subjects

The forces and torques exerted on the handrim during wheelchair propulsion were recorded in five male adult wheelchair users with low-level paraplegia (T12–L1) due to spinal cord injury (SCI) or myelomeningocele (**Table 1**). Subjects provided informed consent and the research protocol was approved by the hospital Institutional Review Board. Each subject had been using a wheelchair as his primary means of mobility for at least 2 years. All subjects used a Quickie II™ (Sunrise Medical, Fresno, CA) manual wheelchair with removable rear wheels. Upon arrival, the subject's weight was measured using a wheelchair scale. The commercial wheels on the subject's wheelchair were removed and replaced with wheels containing instrumented

Table 1.

Subject Code	Age (years)	Height (cm)	Mass (kg)	Level	Cause
DN	37	178	53.1	T12	SCI
KD	36	183	85.3	T12	SCI
JG	37	173	65.8	L1	SCI
JF	24	174	69.0	T12	SCI
SW	32	150	89.4	L1	Myelo
Mean	33.2	171.6	72.5		
S.D.	5.5	12.7	14.9		

handrims. Proper fit of the wheelchair to the user was evaluated by a licensed physical therapist with 10 years of experience treating individuals with paraplegia. In no case did adjustments need to be made to improve fit of the wheelchair to the user.

Data Collection

Reflective markers were placed on the radial and ulnar styloid processes, the lateral aspect of the second MCP joint, and the medial aspect of the fifth MCP. Five trials were collected as the subjects propelled their own wheelchairs using their standard wheelchair propulsion technique along a level runway 3.66 m in length (**Figure 1**). Motion of the markers in three dimensions was recorded at 60 Hz using a six-camera commercial motion analysis system (Motion Analysis Corp., Santa Rosa, CA). Five additional reflective markers were mounted on the wheelchair wheel so that the instantaneous location and orientation of the wheel could be monitored.

The three orthogonal components of force and moment at the wheel axle during propulsion were recorded at 100 Hz using a handrim instrumented with a commercial six-component load cell (JR3, Inc., Woodland, CA). The accuracy of the instrumented handrim for measuring applied force and moment has been previously reported (12). The handrim was mounted to one side of the load cell, and the other side of the load cell was mounted directly to the wheel (**Figure 2**). Therefore, the load cell measured the three orthogonal force and moment components applied to the handrim during propulsion. A miniature data logger was mounted to the wheel to store the load cell voltage data for the duration of each trial. The load cell and motion data were synchronized with a common trigger. After each trial, the data was transferred to a personal computer. The load cell voltage data was converted to force and moment values using a calibration matrix that corrected for any crosstalk between the load cell channels. Baseline data from the

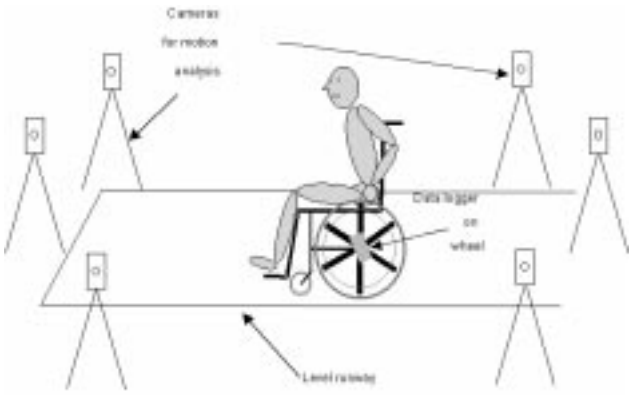

Figure 1.
Schematic of the data collection protocol. Each subject propelled his own wheelchair with the instrumented handrim mounted on the left wheel. Both kinematic and kinetic data are collected simultaneously.

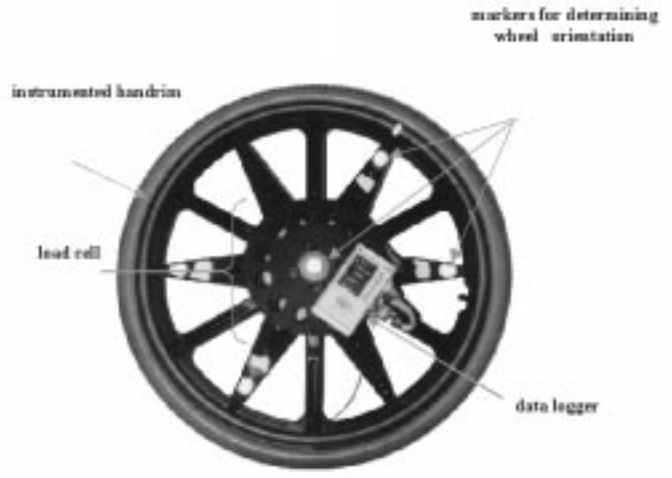

Figure 2.
Data logger mounted on the instrumented handrim.

load cell was collected prior to each data collection session to account for any differences in the attachment of the handrim to the load cell.

Before each data-collection session, the locations of the six cameras were adjusted so that each reflective marker on the subject and the wheelchair could be seen by at least two cameras throughout at least one full propulsion cycle. A view volume, approximately 2 m long × 1 m wide× 2 m high covering the middle 2 m of the runway, was calibrated. The first full-stroke cycle during which the subject was completely within the calibrated volume was chosen for analysis.

The 3-D trajectory data of the markers was smoothed using a generalized cross-validation spline smoothing routine (GCVSPL) with a cutoff frequency of 6 Hz (17). Load cell data were filtered using the GCVSPL routine at a cutoff frequency of 18 Hz, as determined by residual analysis (18). All additional calculations were preformed using custom routines written in Matlab™ (The MathWorks Inc., Natick, MA), which have been validated previously (12). Each analyzable stroke was normalized to percentage-propulsion cycle for subsequent data analysis. The beginning of the stroke cycle was defined as the instant at which any of the three force components became positive (after having been zero during the recovery phase). The end of the propulsion phase was determined in a similar fashion.

Calculations

The components of force and moment applied to the wheel are measured at the wheel axle. However, we are mainly concerned with measuring the resultant force and moment applied at the handrim. The location of the PFA is required to calculate the handrim force and moment components in the r-t-n coordinate system. Once the location of the PFA is known, the handrim force and moment components are calculated from the resultant force and moment measured at the wheel axle and the location of the PFA using the following equations:

$$\begin{aligned} f &= F \\ m &= M - (r \times f) \end{aligned} \qquad [1]$$

where **F** and **M** are the resultant force and moment measured at the wheel center expressed in the global (x-y-z) reference frame; **f** and **m** are the resultant force and moment applied to the handrim; and **r** is the location of the PFA relative to the origin of the global reference frame (**Figure 3**). Once **f** and **m** are known, their tangential, radial, and normal components ($\mathbf{f_t}$, $\mathbf{f_r}$, and $\mathbf{f_n}$) are calculated using the angle ϕ that describes the location of the PFA relative to the horizontal (**Figure 4**). The coordinate axes used in the current study correspond to those used in clinical gait analysis, and do not necessarily coincide with those used by previous authors (13).

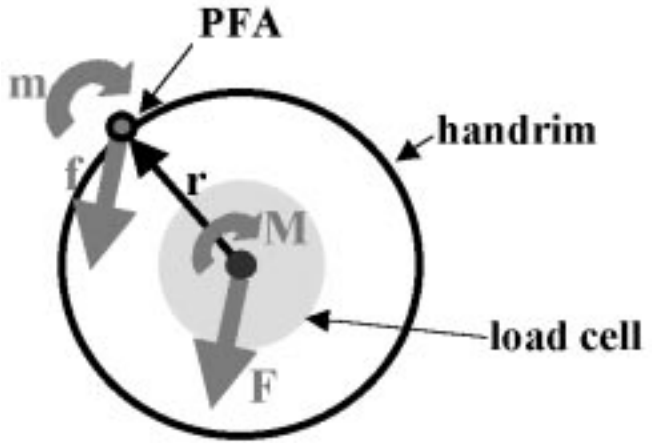

Figure 3.
Relationship between handrim force and moment (**f**,**m**) and the force and moment measured by the load cell at the wheel axle (**F**,**M**).

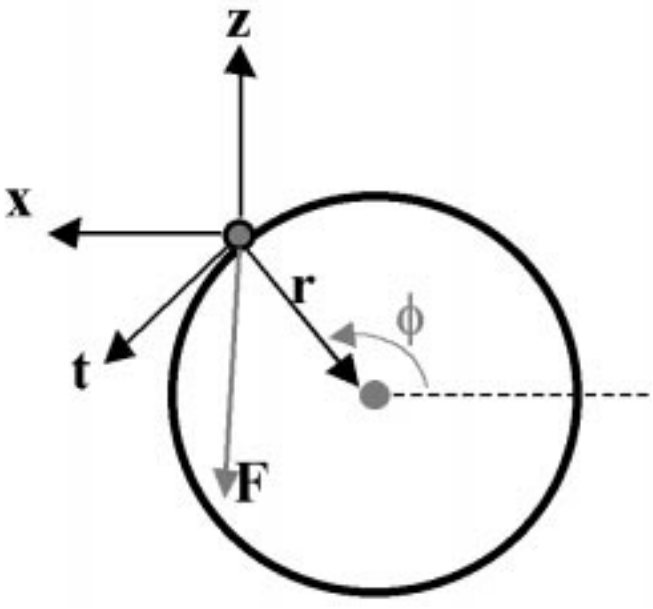

Figure 4.
Definition of the x-y-z (global) coordinate system, the r-t-n coordinate system, and the angle ϕ that defines the location of the PFA. The y-direction points out of the page while the n-direction points inward.

To locate the PFA using kinetic data we must first sum the moments about the load cell center, using the direction conventions shown in **Figure 5**. If the handrim is not located in the same plane as the center of the load cell, the result is the following set of equations:

$$\begin{aligned} M_z &= -F_yR\cos\phi + F_xd + m_z \\ M_x &= -F_yR\sin\phi + F_zd + m_x \\ M_y &= F_xR\sin\phi + F_zR\cos\phi + m_y \end{aligned} \quad [2]$$

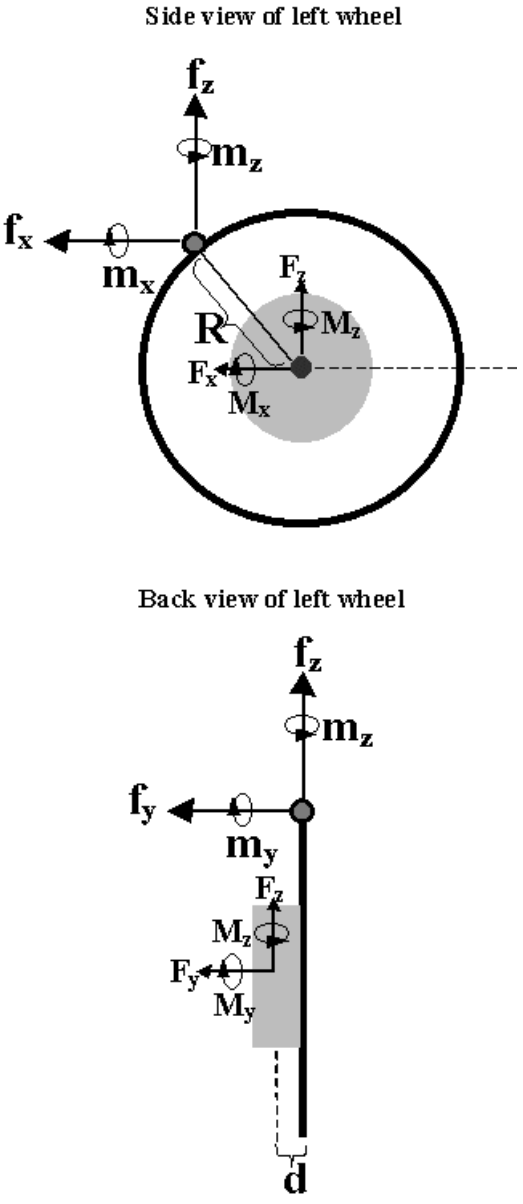

Figure 5.
The forces acting on the wheelchair handrim and definition of the coordinate directions. Wheelchair motion is directed from right to left.

Solving any of these equations for ϕ will yield an equation based solely on the measured forces and moments at the wheel center ($\mathbf{M_x}$, $\mathbf{M_y}$, $\mathbf{M_z}$, $\mathbf{F_x}$, $\mathbf{F_y}$, $\mathbf{F_z}$), the location of the load cell center relative to the handrim (**d**, **R**), and the handrim moment ($\mathbf{m_x}$, $\mathbf{m_y}$, $\mathbf{m_z}$). Because there are four unknowns in the above set of three equations, an additional constraint or assumption is necessary to solve for ϕ. Each equation can be solved for ϕ if the handrim moment component involved is assumed to be zero. Therefore, ϕ, the location of the PFA, can be calculated using any of the following equations:

$$\phi_z = \cos^{-1}\left[\frac{M_z - F_xd}{-F_yR}\right], \text{ assuming } m_z = 0$$

$$\phi_x = \sin^{-1}\left[\frac{M_x - F_zd}{-F_yR}\right], \text{ assuming } m_x = 0$$

$$\phi_{xz} = \tan^{-1}\left[\frac{M_x - F_zd}{M_z - F_xd}\right], \text{ assuming } m_x = m_z = 0$$

$$\phi_y = 2\tan^{-1}\left[\frac{2F_xR \pm \sqrt{F_x^2R^2 - 4\,(M_y^2 - F_z^2R^2)}}{2(M_y - F_zR)}\right],$$

assuming $m_y = 0$ [3]

We calculated ϕ using five different assumptions: (1) $\mathbf{m_z}$=0 (ϕ_z); (2) $\mathbf{m_x}$=0 (ϕ_x); (3) $\mathbf{m_x}$=$\mathbf{m_z}$=0 (ϕ_{xz}); (4) $\mathbf{m_y}$=0 (ϕ_y); and (5) the PFA was located at the second MCP joint (ϕ_{mp}). The value of ϕ_{mp} was calculated by computing the angle of the line joining the second MCP joint and the wheel axle relative to the horizontal. The center of the second MCP was assumed to be located at a point 20 percent of the distance from the center of the second MCP marker to the center of the fifth MCP marker, since these markers were located on the lateral and medial aspects of the MCP joints and not over the joint centers.

If no handrim moment is applied, the values of ϕ_z, ϕ_x, ϕ_{xz}, and ϕ_y should be exactly the same, since the assumptions used in their calculation (that one or more of the handrim moment components is negligible) are valid. Therefore, we would expect the values of ϕ_z, ϕ_x, ϕ_{xz}, and ϕ_y to be similar in a "no moment" condition. Differences between ϕ_z, ϕ_x, ϕ_{xz}, and ϕ_y give insight into which assumptions were violated. For example, if ϕ_z, ϕ_x, and ϕ_{xz} are sim-

ilar but ϕ_y varies significantly from the other three, it is likely the assumption $\mathbf{m}_y$=0 that was used to calculate ϕ_y is invalid, while the assumptions that $\mathbf{m}_x$=0 and $\mathbf{m}_y$=0 used to calculate ϕ_z, ϕ_x, and ϕ_{xz} are likely valid.

To quantify differences in the calculated PFA location due to the assumptions, the lag or lead of ϕ_z, ϕ_x, ϕ_{xz}, and ϕ_y relative to ϕ_{mp} was calculated at each 2 percent of the propulsion phase. The value of ϕ_{mp} was chosen as the reference because its value is stable throughout the propulsion cycle, and it has been used previously to define the location of the PFA (5,10,11). A positive value of lag describes a situation where ϕ_{mp} is greater than the variable of interest, a negative value means ϕ_{mp} is less than the variable of interest. The range of ϕ values at each 2 percent of the propulsion phase was also calculated as an indication of the similarity of the values calculated with the different assumptions. In addition, the resulting handrim force and moment components were calculated using all five ϕ values at each 2 percent of the stroke cycle. The *e*, sometimes referred to as fraction effective force or FEF (16), was calculated for the mean strokes using each of the five assumptions to evaluate the effects of style and assumption on the resulting mechanical *e*. The *e* was calculated using the following formula:

$$e = \frac{F_t}{|F|} \qquad [4]$$

Therefore, when the tangential component of force was directed positively, *e* was positive. However, if it was in a negative direction (hindering forward motion of the wheel), the *e* could be negative. Because *e* is the ratio of the tangential force component to the resultant force, and the location of the PFA determines the relative magnitudes of the force components, the location of the PFA affected the calculated *e* value.

Data from five trials for each subject were averaged to provide mean angle, force, lag/lead, range, and *e* curves for each subject in each condition. The subject averages were used to create ensemble mean curves for each condition across the entire subject pool. Comparisons of the ensemble means between conditions were made to compare the angle, force, moment, and *e* between the two stroke conditions.

RESULTS

The values of ϕ_z, ϕ_x, ϕ_{xz}, and ϕ_y were quite variable at the beginning and end of the propulsion phase (**Figure 6**). In these two regions the force and moment values measured at the wheel axle were very small (**Figure 7**). Because the ϕ values are calculated using a ratio of force and moment values, the calculations become unstable at these times. Therefore, the first and last 20 percent of the propulsion phase were not included in subsequent comparisons. Such a phenomenon has been described previously (13,14,15). In contrast, ϕ_{mp} was very stable and repeatable throughout the propulsion phase in all cases.

Even in the middle portion of the propulsion phase the values of ϕ_z, ϕ_x, ϕ_{xz}, and ϕ_y varied greatly from each other (**Figure 6**), indicating that not all the assumptions were valid. In some trials, all five values of ϕ could not be calculated because the equations led to a value of sine or cosine that was greater than 1 or less than −1, again indicating the assumptions used in their formulation were invalid.

The mean lag values for ϕ_z, ϕ_x, ϕ_{xz}, and ϕ_y were 9.7±7.2˚, 24.7±7.1˚, 5.4±4.0˚, and 12.7±11.9˚, respectively (**Figure 8**). The mean range of all ϕ values was 23.9±7.4˚ and the range of ϕ_z, ϕ_x, and ϕ_{xz} was slightly less, averaging 19.6±5.5˚.

The *e* generally increased throughout the middle portion of the propulsion phase, peaking at approximately 0.80 three-quarters of the way through the propulsion phase (**Figure 9**). However, the choice of ϕ value greatly affected the computed *e*. The *e* values calculated using ϕ_z and ϕ_{xz} were similar (differing by no more than 0.05), and closely followed the data from ϕ_{mp} during the majority of the propulsion phase. The *e*values calculated with ϕ_x and ϕ_y were quite a bit lower early and late in the propulsion cycle, respectively.

The radial force component values were similar for ϕ_z, ϕ_{xz}, and ϕ_{mp} throughout the majority of the propulsion cycle (**Figure 10a**). Values calculated using ϕ_y and ϕ_x were quite different from the other three values, especially between 30 percent and 70 percent of the propulsion phase. The tangential force components were also similar for ϕ_z, ϕ_{xz}, and ϕ_{mp}, although the values for ϕ_{mp} tended to be greater throughout the propulsion phase (**Figure 10b**). The values calculated using ϕ_x and ϕ_y varied greatly from the other values, throughout the majority of the propulsion cycle. Normal force components were practically identical regardless of the assumptions used in their calculation (**Figure 10c**).

The radial and tangential components of the handrim moment were generally less than 1 Nm in magnitude (**Figures 11a** and **b**). The values of the radial component calculated using ϕ_z and ϕ_{xz} were similar, and

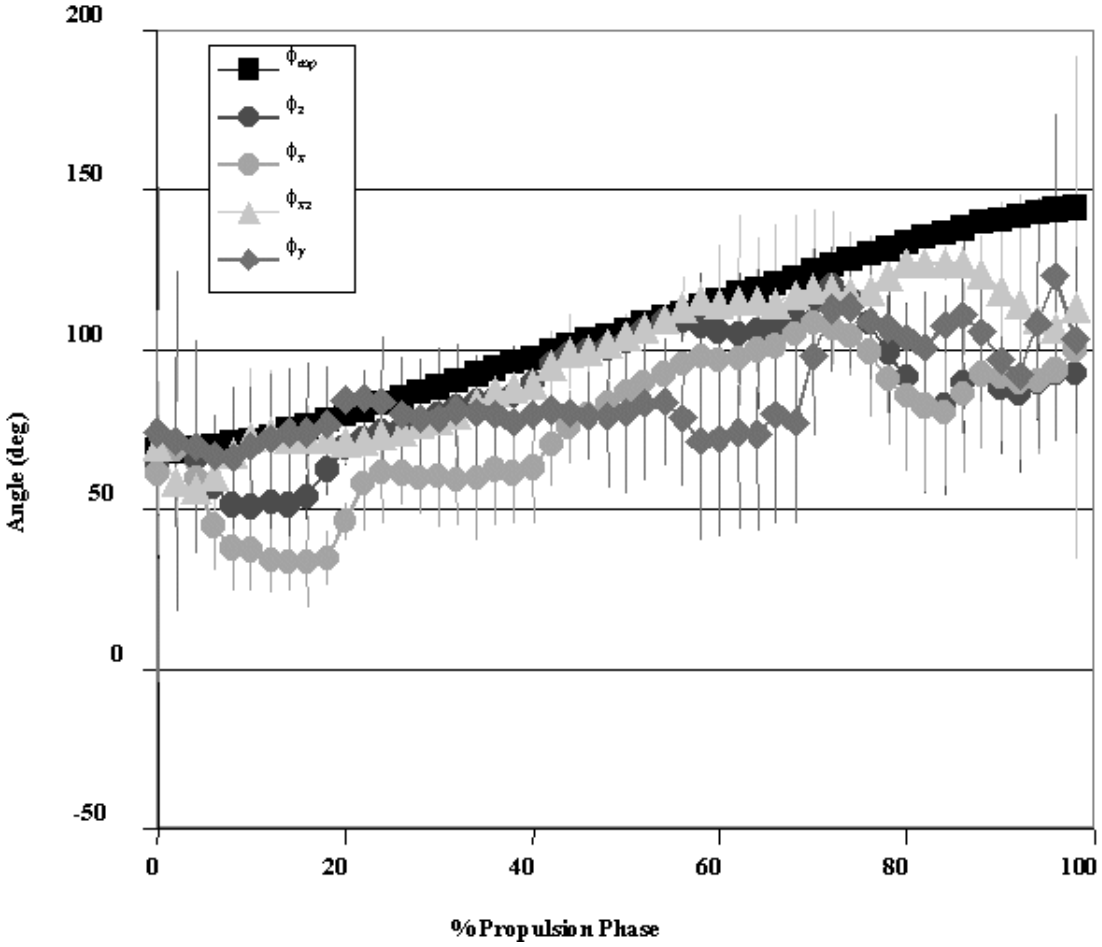

Figure 6.
The PFA location for trials of one subject. Values shown are mean (solid lines) ±S.D. (dotted lines). The PFA locations for ϕ values calculated with kinetic data were quite variable, especially during the initial and final portions of the stroke phase.

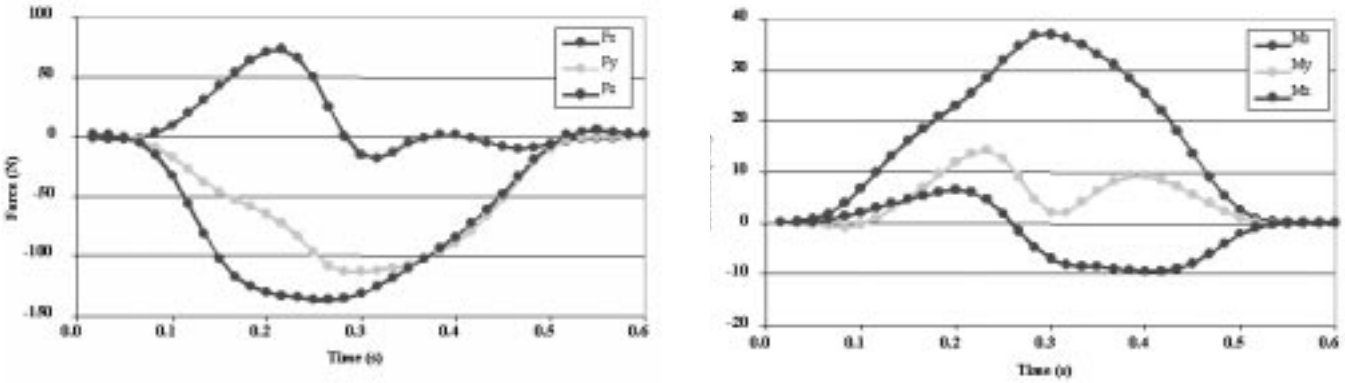

Figure 7.
Forces (A) and moments (B) measured at the wheel center during a representative trial. Both the forces and moments are close to zero near the beginning and end of the propulsion phase.

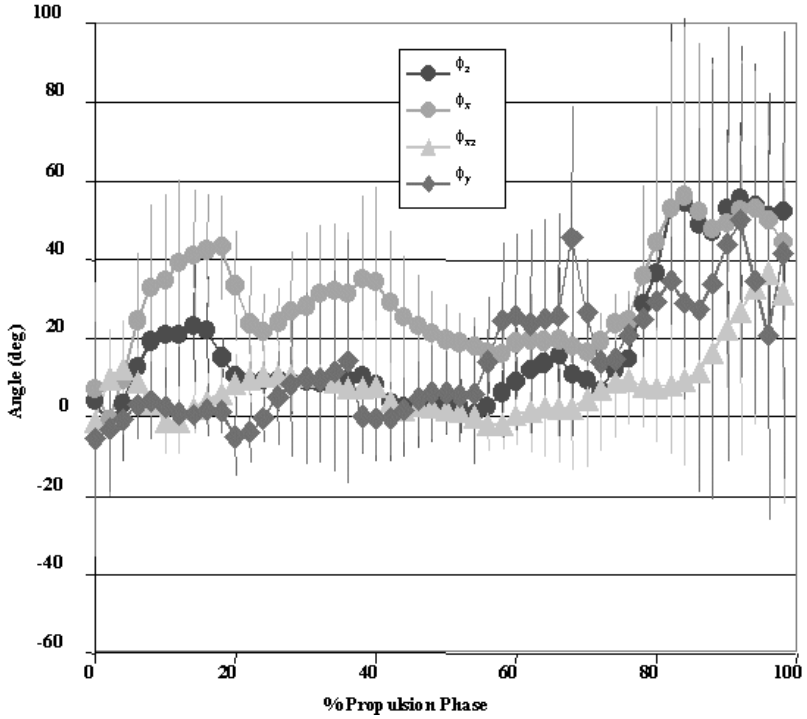

Figure 8.
Mean lag values (solid lines) ±S.D. (dotted lines) for all trials. A positive value means the variable of interest lags the second MCP joint. The ϕ values varied widely throughout the stroke cycle, suggesting that the assumptions used in their calculation were violated.

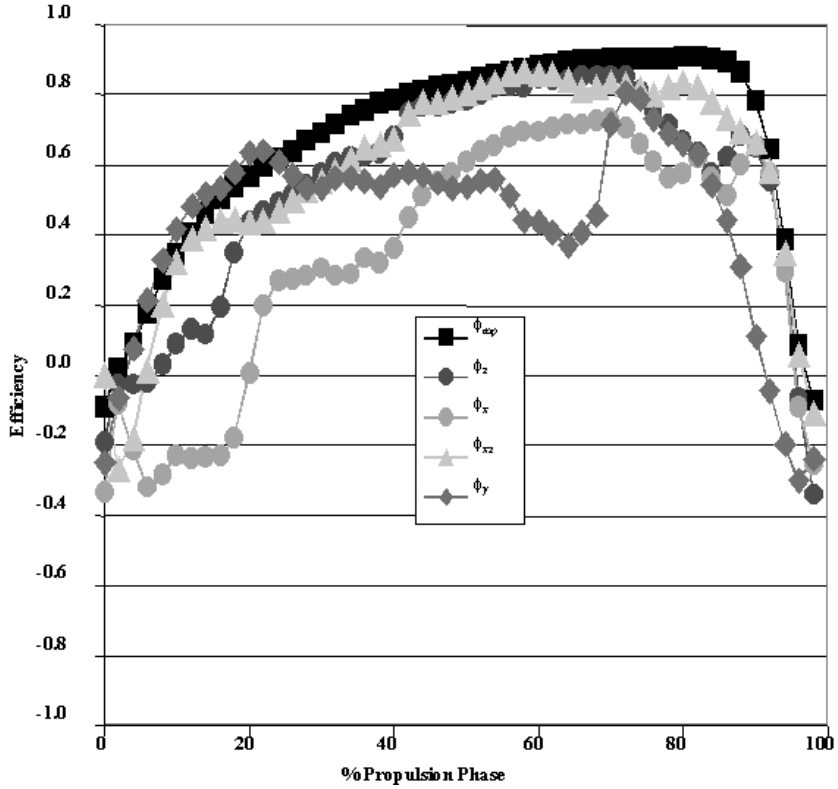

Figure 9.
Mean *e* values for all trials. Efficiency values varied widely depending on the assumptions used in their calculation.

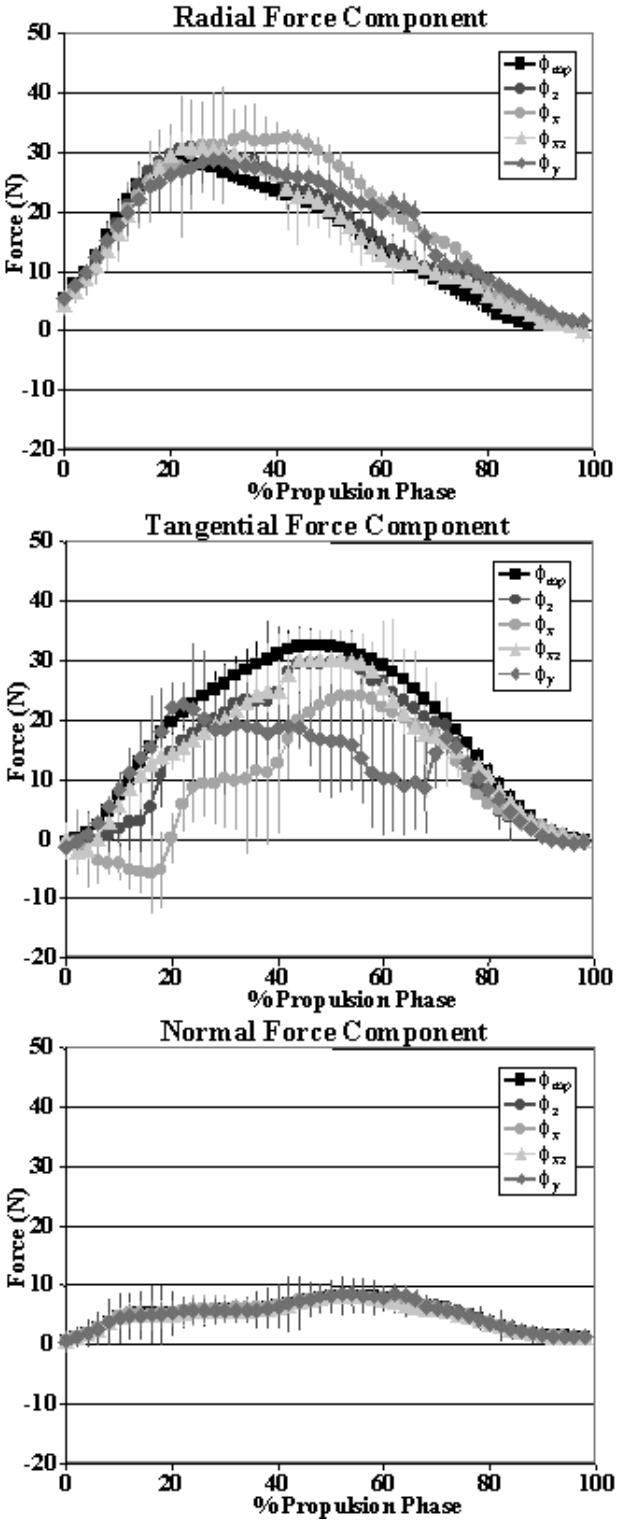

Figure 10.
Mean radial (A), tangential (B), and normal (C) components of handrim force. Values shown are mean ±S.D. (dotted lines).

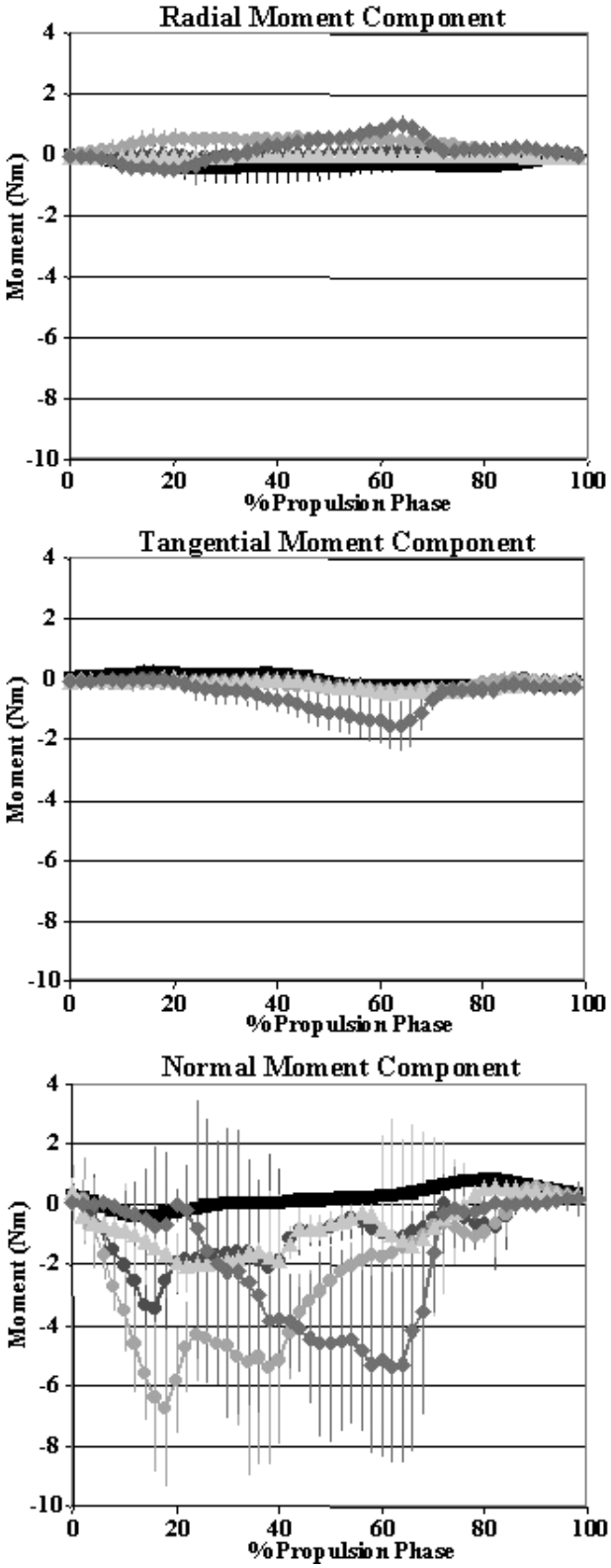

Figure 11.
Mean radial (A), tangential (B), and normal (C) components of handrim moment. Values shown are mean ±S.D. (dotted lines).

approximately equal to zero. Values calculated using ϕ_{mp} were slightly less than zero, while values calculated using ϕ_x and ϕ_y were slightly greater than zero. The tangential moment component calculated using ϕ_y was negative in the middle portion of the propulsion cycle, while values calculated with all other methods were essentially zero.

The normal moment component was extremely variable for all calculations using kinetic data, as evidenced by the large standard deviations (S.D.) for these variables (**Figure 11c**). The mean values of ϕ_z, ϕ_x, ϕ_{xz}, and ϕ_y were generally less than zero, while the data calculated using ϕ_{mp} was approximately equal to or slightly greater than zero.

DISCUSSION

Scientists studying the biomechanics of wheelchair propulsion are faced with the dilemma of choosing a method to compute the location of the PFA. On the one hand, methods utilizing a fixed point on the hand involve simple calculations from kinematic data and are stable throughout the propulsion cycle, but likely oversimplify the problem of identifying the PFA. On the other hand, using kinetic data to solve for the PFA location is appealing, but the effects of the underlying assumptions are not well quantified and the PFA location is unstable. In addition, there are several potential methods to be used to compute the location of the PFA, and their individual strengths and weaknesses have not been compared. The purpose of this study is to provide data to allow investigators to make an informed decision when choosing a technique for calculating the location of the PFA.

Cooper et al. (19) were the first authors to propose the use of the PFA or center of pressure to analyze manual wheelchair propulsion technique. They felt that the location of the PFA could potentially be used as a diagnostic tool to identify wheelchair users at high risk for ailments such as carpal tunnel syndrome. Their initial study located the PFA in three planes through the hand that were parallel with the anatomic planes, and noted that the PFA was not generally coincident with any anatomical marker (19). In a followup study, Cooper et al. (13) compared the kinetic data and kinematic data techniques for locating the PFA on one subject and recommended the use of kinetic data over kinematic data. However, the effects of different calculation methods using kinetic data on PFA location and stability were not quantified. In addition, the conclusions were drawn based on the data of a single subject, so the effects of different propulsion techniques due to differences in size, strength, experience, and wheelchair fit on PFA calculations could not be addressed.

In the current study, we have supplemented the existing data by evaluating five different methods for locating the PFA in a "normal" situation where subjects used their own natural techniques. This way, the differences in location of the PFA due to calculation method could be compared in realistic circumstances. However, there is still no gold standard with which to compare the data, so it has been assumed that similarities in data are due to the underlying assumptions of the equations producing the data being met or nearly met. Another limitation of this study is that it involves only five subjects, all of who were male. Therefore, it is likely that some propulsion styles were not included in this analysis. Differences in propulsion style could result due to size, strength, and fitness differences between male and female subjects.

The values of ϕ_z, ϕ_x, ϕ_{xz}, and ϕ_y were often unstable, and varied greatly depending on the subject. In fact, for each subject, certain calculation methods were less stable than others, resulting in equations that could not be solved, but there was no identifiable pattern to the instability. The variable ϕ_y was unstable in the largest number of subjects, however, suggesting that handrim moments about the axis of the wheel are generated, and are significant enough to affect calculations. Handrim moments have previously been shown to be approximately an order of magnitude less than the moment of force about the wheel axis (20); however, we have shown they can affect calculations of the location of the PFA.

The most likely explanation for the instability of certain variables in certain subjects is that the handrim moment components are highly individual, and depend on the strength, technique, and physique of the individual. Therefore, consistently using one set of assumptions to locate the PFA for several subjects may lead to substantial errors. However, some calculation methods did prove to be more stable than others, suggesting they should be used in the general case.

The mean values of ϕ_z and ϕ_{xz} were similar in the middle portion of the propulsion phase for all of the variables of interest. Therefore, assuming $\mathbf{m}_z=0$ or $\mathbf{m}_x=\mathbf{m}_z=0$ appears to be reasonable for most subjects. In fact, ϕ_{xz} was the most stable of any of the variables calculated using kinetic data. While at first glance it seems unlikely that ϕ_{xz} would be a better choice than either ϕ_z or ϕ_x

since it involves two assumptions that must be satisfied at all times, the equation used to calculate ϕ_{xz} is more stable numerically than the others since it involves only force and moment components in the x- and z-directions. The formulas for ϕ_z and ϕ_x both contain $\mathbf{F}_y$ in the denominator, which tends to be small and variable, resulting in computational difficulties and instability.

The lag/lead data presented in the current study supports the previous work of Cooper and colleagues which demonstrated that PFA does not remain at a consistent location within the hand during propulsion (13,14,19,20). While the PFA location calculated with ϕ_{xz} was close to ϕ_{mp} on average (lag 5.4±4.0˚), the range of lag values was from −2.0˚ to 10.4˚. In short, the most consistent PFA calculation led the second MCP joint at times, and lagged it by over 10˚ at other times.

The *e* values calculated using ϕ_z and ϕ_{xz} were generally similar and tended to follow the values calculated using ϕ_{mp}. Therefore, assuming the location of the PFA at the second MCP joint does not seem to greatly affect *e* values. In general, *e* calculated assuming the PFA is located at the second MCP joint tends to overestimate the true *e* values slightly.

When calculating the handrim force components, the assumptions have no effect on the normal component of force, but do alter the values of $\mathbf{F}_r$ and $\mathbf{F}_t$ slightly. Using ϕ_z, ϕ_{xz}, or ϕ_{mp} resulted in very similar values of $\mathbf{F}_r$, but $\mathbf{F}_t$ was greater throughout much of the stroke when ϕ_{mp} was used than when ϕ_z or ϕ_{xz} were used. The increased value of F_t results in the increased *e* values calculated with ϕ_{mp} compared to those calculated with ϕ_z or ϕ_{xz}, as noted above. Handrim moment components about axes other than the wheel axis were negligible, at least in this population of subjects who propelled their wheelchairs without the use of gloves or high-friction handrims (the handrims were aluminum). The handrim moments produced about the wheel axis were opposite the direction of progression, and therefore tended to hinder progress of the wheelchair.

Cooper et al. (13) suggested that PFA be calculated from kinetic data for the most accurate results. While this is true, it has not been clear which calculation method should be used to calculate PFA from the kinetic data. The current study demonstrates that the assumption that m_y is negligible was invalid in nearly all subjects. The assumptions that other handrim moment components were negligible were not consistently valid. Using the second MCP joint to locate the PFA leads to stable values throughout the propulsion cycle, but will generally lead to higher values of ϕ than the other methods. Therefore, the relative strengths and weaknesses of each technique must be weighed for the particular study. Location of the PFA is important for determining the handrim force and moment components and the resulting mechanical *e* calculations. However, it is not needed to compute the upper-limb joint forces and moments in wheelchair propulsion, which can be done using the force and moment data measured at the wheel center. Therefore, the choice of methods used to locate the PFA will not affect many of the important biomechanical variables in wheelchair propulsion.

We have shown that the assumptions used to calculate the location of the PFA greatly affect the results and any subsequent calculations made using the PFA, such as the mechanical *e* and the magnitude of the handrim force components. Different assumptions appeared to be appropriate for different subjects, so no one method of computing the PFA location is ideal. If kinetic data are used to locate the PFA, using ϕ_{xz}, or the assumption that $\mathbf{m}_x=\mathbf{m}_z=0$, was the most stable and realistic means of calculating PFA. This is not surprising, since the out-of-plane moments are not expected to be large in wheelchair propulsion. Assuming the PFA is located at the second MCP joint leads to some minor inaccuracies in the computation of handrim force and moment components, but also results in stable data throughout the propulsion phase. Ideally, a force and moment transducer with redundant measurements at different locations will be developed to solve for the location of the PFA explicitly, avoiding the use of assumptions.

ACKNOWLEDGMENTS

Special thanks to Emily Shin, Diana Hansen, and Brian Kotajarvi for their help with data collection and analysis.

REFERENCES

1. Gellman H, Sie I, Waters RL. Late complications of the weight bearing upper extremity in the paraplegic patient. Clin Orthop 1988:233:132–5.
2. Nichols PJR, Norman PA, Ennis JR. Wheelchair user's shoulder?: shoulder pain in patients with spinal cord lesions. Scand J Rehabil Med 1979:11:29–32.
3. Bayley JC, Cochran TP, Sledge CB. The weight-bearing shoulder: the impingement syndrome in paraplegics. J Bone Joint Surg Am 1987:69(5):676–8.

4. Sie IH, Waters RL, Adkins RH, Gellman H. Upper extremity pain in the postrehabilitation spinal cord injured patient. Arch Phys Med Rehabil 1992:73:44–8.
5. Veeger HEJ, van der Woude LHV, Rozendal RH. Load on the upper extremity in manual wheelchair propulsion. J Electromyog Kines 1991:1(4):270–80.
6. Robertson RN, Boninger ML, Cooper RA, Shimada SD. Pushrim forces and joint kinetics during wheelchair propulsion. Arch Phys Med Rehabil 1996:77:856–64.
7. Boninger ML, Cooper RA, Robertson RN, Shimada SD. Three-dimensional pushrim forces during two speeds of wheelchair propulsion. Am J Phys Med Rehabil 1997:76:420–6.
8. Asato KT, Cooper RA, Robertson RN, Ster JF. SMART^{Wheels}: development and testing of a system for measuring manual wheelchair propulsion dynamics. IEEE Trans Biomed Eng 1993:40(12):1320–4.
9. VanSickle DP, Cooper RA, Robertson RN. SMART^{Wheel}: development of a digital force and moment sensing pushrim. In: Proceedings of the 18th International RESNA Conference, Vancouver, BC, Canada. Washington, DC: RESNA Press 1995:352-4.
10. Su FC, Lin LT, Wu HW, Chou YL, Westreich A, An KN. Three-dimensional dynamic analysis of wheelchair propulsion. Chinese J Med Biol Eng 1993:13(4):329–42.
11. Rodgers MM, Gayle GW, Figoni SF, Kobayashi M, Lieh J, Glaser RM. Biomechanics of wheelchair propulsion during fatigue. Arch Phys Med Rehabil 1994:75:85–93.
12. Wu HW, Berglund LJ, Su FC, Yu B, Westrich A, Kim KJ, An KN. An instrumented wheel for kinetic analysis of wheelchair propulsion. J Biomech Eng 1998:120:533–5.
13. Cooper RA, Robertson RN, VanSickle DP, Boninger ML, Shimada SD. Methods for determining three-dimensional wheelchair pushrim forces and moments: a technical note. J Rehabil Res Dev 1997:34:162–70.
14. Cooper RA, Robertson RN, VanSickle DP, Boninger ML, Shimada SD. Projection of the point of force application onto a palmar plane of the hand during wheelchair propulsion. IEEE Trans Rehabil Eng 1996:4:133–42.
15. Cooper RA, Boninger ML, VanSickle DP, Robertson RN, Shimada SD. Uncertainty analysis for wheelchair propulsion dynamics. IEEE Trans Rehabil Eng 1996:5:130–9.
16. Veeger HEJ, van der Woude LHV, Rozendal RH. Load on the upper extremity in manual wheelchair propulsion. J Electromyog Kines 1991:1:270–80.
17. Woltring HJ. A fortram package for generalized, cross-validatory spline smoothing and differentiation. Adv Eng Software 1986:8:104–13.
18. Winter DA. Biomechanics and motor control of human movement (second edition). New York: John Wiley & Sons, Inc.; 1990. p. 41–3.
19. Cooper RA, VanSickle DP, Robertson RN, Boninger ML, Ensinger GJ. A method for analyzing center of pressure during manual wheelchair propulsion. IEEE Trans Rehabil Eng 1995:3:289–98.
20. VanSickle DP, Cooper RA, Boninger ML, Robertson RN, Shimada SD. A unified method for calculating the center of pressure during wheelchair propulsion. Ann Biomed Eng 1998:328–36.

Submitted for publication February 9, 1999. Accepted in revised form May 18, 2000.